

In vitro osteoclast formation and resorption of silicon-substituted hydroxyapatite ceramics

Robert J. Friederichs^a, Roger A. Brooks^b, Masato Ueda^c, Serena M. Best^a

^a *Department of Materials Science & Metallurgy, University of Cambridge, 27 Charles Babbage Road, Cambridge, CB3 0FS, UK*

^b *Division of Trauma & Orthopaedic Surgery, Box 180, Addenbrooke's Hospital, Hills Road, Cambridge, CB2 0QQ, UK*

^c *Department of Chemistry & Materials Engineering, Faculty of Chemistry, Materials & Bioengineering, Kansai University, 3-3-35 Yamate-cho Suita Osaka 564-8680, Japan*

ABSTRACT

Materials that participate in bone remodelling at the implant / tissue interface represent a modern tissue engineering approach with the aim of balancing implant resorption and nascent tissue formation. Silicon-substituted hydroxyapatite (SiHA) ceramics are capable of stimulating new bone formation, but little is known about their interaction with osteoclasts (OC). The effects of soluble silicate and SiHA on OCs were investigated in this study. Soluble silicate below 500 mM did not stimulate cell metabolism at 4 days or alter resorption area at 7 days on calcium phosphate discs. On sintered ceramics, OC numbers were similar on HA, Si_{0.3}HA (0.5 wt%Si) and Si_{0.5}HA (1.2 wt%Si) after 21 days *in vitro*, but actin ring sealing zone morphology on SiHA resembled that commonly found on bone or on carbonate-substituted hydroxyapatite (CHA). Smaller and thicker actin rings on SiHA compared to HA were probably the result of altered surface chemistry and solubility differences. The more stable sealing zones and increased lattice solubility likely contributed to increased individual pit volumes observed on Si_{0.5}HA. The delayed formation of OCs on Si_{0.5}HA (lower numbers at day 14) excludes earlier differentiation as a possible mechanism of increased individual OC pit volumes at later times (day 21). Materials characterization of Si containing biomaterials remains paramount as the Si type and amounts can subsequently impact downstream OC behaviour in a complex manner.

KEYWORDS:

Hydroxyapatite, Silicon (silicate), osteoclast, resorption, pits, calcium phosphate

INTRODUCTION

Bone is a dynamic structure that undergoes extensive remodelling via osteoclastic (OC) resorption and new tissue formation by osteoblasts (OB). Increased calcium phosphate (CaP) resorption by OCs may allow for more bone tissue production when both resorption and bone formation are in homeostasis. Studies on bovine cortical bone and synthetic carbonate-substituted hydroxyapatite (CHA) have suggested that OC resorption may stimulate subsequent OB activity or even bone forming ability.¹⁻³ However, remodelling is known to occur *in vivo* at plasma-sprayed HA surfaces that leads to a gradual loss of the ceramic coating.^{4,5} Silicon-substituted HA (SiHA) has had success *in vivo* as a synthetic bone-grafting material, but the mechanism of increased osteoconduction seen with this material is not well understood.⁶ Active remodelling of SiHA was suspected as a mechanism for enhanced bone formation in a study by Hing et al. where porous SiHA (0.8 wt%) was implanted in a lapine model for 12 weeks.⁷ The proposed involvement of remodelling in bone formation around implants has led to more researchers investigating the effects of biomaterials on OCs. Techniques such as RT-PCR (mRNA expression), histological staining (TRAP), fluorescence microscopy of OC sealing zones and 3D characterisation of resorption pits have all revealed materials induced OC responses.⁸⁻¹²

Higher dissolution rates from SiHA compared to HA may contribute to the success of SiHA as a bone graft material.¹³ However, the effect of soluble and lattice bound Si on OCs remains unclear. Soluble silicate ions [3-100 μM] did not show any stimulatory effects on RAW 264.7 OCs after 3 days in the presence of SaOS-2 osteosarcoma cells.¹⁴ More recently, Mladenović et al. reported that the degradation products of bioglass 45S5 (orthosilicic acid) inhibited *in vitro* phenotypic gene expression, OC formation and resorption of murine cavariar bone.¹⁵ They found a lower limit of $\sim 690 \mu\text{M}$ inhibited OC resorption activity. Studies

correlating these findings to SiHA are rare, but some groups have investigated OC formation and activity on SiHA.

Botelho et al. first studied the OC response to SiHA using CD14+ peripheral human blood monocytes (PBMC).¹¹ Actin and vinculin were visualised around OC sealing zones at 21 days and increased Ca and P release was seen from SiHA (1.5 wt%), but not HA. Lehmann et al. found a wider range of OC lacunae diameters on biphasic α -tricalcium phosphate (TCP) / SiHA (1.4 wt% Si) compared to HA at 21 days, but the role of silicon was unclear due to the presence of TCP.¹⁶ Contrary to these studies, Matesanz et al. found inhibited *in vitro* OC development and reduced resorption on nano grained nSiHA (~0.8 wt% Si) discs calcined at 700 °C compared to nano grained nHA at 21 days.¹⁷ However, their functional *in vitro* OC resorption study was limited to resorption pit diameter measurements. More work is needed to clarify OC resorption activity on well-characterized SiHA substrates.

A more detailed study of OC activation may provide more evidence for the effects of silicon. Quantitative measurement of actin ring morphology might indicate OC sealing zone stability,¹⁸ and area measurement of resorption pits, while useful, may not adequately describe OC resorption activity because of differences in pit depth.^{9,10} The goals of this study were to determine 1) whether soluble silicate, in the presence of RANKL, increased OC resorption of CaP coated culture wells, 2) if OC formation on SiHA was enhanced or reduced compared to HA and 3) if SiHA altered OC resorption compared to HA. The number of OCs, the morphology of sealing zones and resorption pits was also determined.

MATERIALS AND METHODS

Materials preparation

HA powder (Ca/P ratio 1.667) was prepared using the calcium hydroxide / orthophosphoric acid based aqueous wet precipitation method of Jarcho.¹⁹ SiHA (0.8 and 1.5 wt% (x=0.3 and 0.5 in Equation 1) with calculated Ca/P ratios of 1.750 and 1.812 respectively) was prepared using similar methods, but tetraethylorthosilicate (TEOS, 86578, Sigma Aldrich, UK) was added to the calcium hydroxide solution prior to the addition of diluted H₃PO₄.^{20,21} The molar calcium amount was decreased by 1% below the calculated Ca/P ratios for SiHA in order to retain phase purity and subvert the formation of CaO. HA and SiHA powders were ground in an alumina crucible and mechanically sieved below 75 µm before uniaxial pressing in a 13 mm die at 75 MPa. Discs were then sintered at 1200 °C for 2 hours and ground to a 15 µm (P1200) finish with SiC paper before sterilisation by steam autoclave. Sintered disc diameters were ~9.6 mm in diameter and ~2 mm thick with theoretical densities >98%.



Materials characterisation

The phase structure of HA and SiHA powders heated to 1200 °C was examined using X-ray diffraction (XRD). A Philips PW1050 diffractometer (PANalytical, NL) with monochromatic Cu K α radiation was used to scan over a range of 25-50° 2 θ and Philips HighScore plus software was used to match peaks to appropriate International Centre for Diffraction Data (ICDD) files such as HA 09-0432, CaO 37-1497, α -TCP 29-0359 and β -TCP 70-2065. Fourier transform infrared spectroscopy (FTIR) was performed on heat-treated powders (1200 °C) using a Bruker Tensor 27 in transmission mode (KBr pellets) over the range of 400-4000 cm⁻¹. X-ray fluorescence (XRF) analysis of HA and SiHA was outsourced to LSM Analytical (UKAS 1091,

UK). 15 different elemental oxides were measured including Ca, Si and P with minimum detection limits of 0.05 wt%.

CD14+ monocyte isolation and OC culture

The isolation of CD 14+ peripheral blood monocytes (PBMC) was based on the methods reported by Schilling, Spence and Botelho et al.^{11,12,22} Whole blood was obtained from a healthy donor who gave written consent to the Orthopaedic Research Unit, University of Cambridge under Local Research Ethics Committee agreement 06/Q0108/213. The procedure of Botelho et al. was followed, and CD14+ PBMCs were isolated and suspended in α -Minimum essential medium (MEM) (41061 Gibco, Invitrogen, UK) supplemented with heat inactivated 10% AB human male serum (CS400 HD Supplies, TCS Biosciences, UK), 1% v/v penicillin, streptomycin, glutamine (10 units.ml⁻¹ penicillin, 10 μ g.ml⁻¹ streptomycin, 29.2 mg.ml⁻¹ glutamine, 10378, Gibco) and ascorbic acid (30 μ g ml⁻¹).

The CD14+ PBMCs were counted using a Cell Scepter (Millipore), diluted to the desired concentration and seeded in a bead of 67 μ l of media per disc at 3,865 cells.mm⁻² on ceramic discs or into the wells of Ostellogic CaP-coated slides at 5 x 10⁴ cells.well⁻². The samples were incubated in a humidified atmosphere containing 5% CO₂ at 37 °C for 2 hours. Afterwards the wells were flooded with α MEM supplemented with 50 ng mL⁻¹ RANKL (recombinant human soluble RANK ligand, 10-1141, Insight Biotech., UK) and 25 ng mL⁻¹ of recombinant human macrophage colony stimulating factor (M-CSF, 216-MC, R&D systems, UK). Each ceramic disc had 1.0 ml of medium that was changed once every 7 days.

Sodium silicate preparation

A batch of sodium silicate solution (Sigma-Aldrich 338443) with a Si concentration of 13.1% (gravimetric assay) and a titrated NaOH level of 13.7% was diluted to give in culture medium to give silicon concentrations of 0.005 – 500 μ M silicon. 13.7% NaOH solution (Sigma) was diluted in deionised water to in the same way to give equivalent NaOH concentrations as control solutions. Commercially available CaP coated discs (BD Biocoat Osteologic, BD Biosciences, UK) were used as substrates to test whether soluble silicate altered OC resorption behaviour. Silicate or NaOH solutions were added to the Osteologic slides 5 days after monocyte seeding when multinucleate cells were visible.

MTS assay

An MTS assay was used according to the manufacturer's protocol to determine the viability of cells on Osteologic discs 3 days after the addition of silicate (CellTiter 96[®] AQueous cell proliferation assay, Promega).

Quantifying calcium phosphate resorption

The effect of soluble silicon on the resorption of calcium phosphate was determined 3 days after the addition of silicate. Medium was removed from the Osteologic wells and the cells removed by treating with 1% v/v NaOH for 1 hour. Cells were rinsed thoroughly with de-ionised water and the remaining calcium phosphate stained using the von Kossa method. 5% w/v silver nitrate solution was added for 30 minutes and after rinsing the colour was developed with 5% w/v sodium thiosulphate. Discs were rinsed, dried and resorbed areas determined by capturing an image of each well area using a Leitz Dialux 20 microscope (Leica) and a Retiga Exi camera (QImaging). Areas were measured using PCImage software (Synoptics).

TRAP staining

TRAP has been associated with OCs and active bone resorption, but other cells (such as osteocytes or some mononuclear cells) are also known to stain positive for TRAP.²³ Therefore, TRAP staining was performed at 21 days with the addition of fluorescent imaging of actin rings and multinucleated cells to differentiate OCs from other cell types. The TRAP staining procedure as described in Farquharson et al. was used to stain CD14+ PBMCs grown on pernanox sides for 21 days.²⁴

Fluorescent microscopy-actin and nuclei staining

Fluorescence microscopy was performed on samples at days 14 and 21 on SiHA and HA. The cells were washed twice with PBS and fixed in 4% paraformaldehyde solution for 10 minutes. Cells were stained using immunocytochemistry techniques similar to those used by Botelho et al. where phalloidin TRITC (Sigma Aldrich, UK) diluted 1:1000 in 1% BSA-PBS solution was used to stain for F-actin and Vectashield mountant containing 4',9-diamidino-2-phenylindole dihydrochloride (DAPI) anti-fade mounting agent (Vector Labs, UK) stained the nuclei.¹¹ A Leica DMRXA 2 fluorescence microscope was used in conjunction with Surveyor (Objective imaging version 5.5.5.30) software with an Oasis automation control system in order to create a fluorescent mosaic image of the entire sample taken at 10 X magnification. OC counting was performed using Image J (NIH, USA) with the cell-counter plug in. An OC was defined as having 3 or more nuclei (fluoresced blue) and an actin ring (fluoresced red). Actin ring diameters and thicknesses were measured (50 each per sample) near the centre of the discs where OCs were confluent.

2-dimensional imaging of OC resorption pits

Resorbed surfaces at days 11 and 21 were gently cleaned and placed in an ultrasonic bath to remove cellular material. Dried discs were sputter coated with gold (Emitech 550) and imaged using a JEOL 820 scanning electron microscope (SEM) at an accelerating voltage of 10 kV. Stereoscopic light microscopy was also performed and the gold coatings increased contrast between resorbed / native surfaces. Image J was used to convert the images to black and white then a threshold was set by hand to reflect the resorbed area.

3-dimensional microscopy of OC resorption pits

A 3D laser colour microscope (VK-9500, Keyence, Japan) was used to measure resorption pit volumes within a region of interest (ROI). Win-ROOF 3D software (Mitani Corp., Japan) was used to process a mosaic of images (~300 per sample). First, any sample sloping from uneven polishing was corrected using a software algorithm. A baseline volume was measured on the as polished discs for comparison to the resorbed samples to show that the volume of resorption was not a measurement artefact. A 5 mm diameter ROI was selected in an area containing resorption pits, and the threshold was set using the laser light images manually with good repeatability. 3 ROIs were measured per sample, and n=5 samples per condition were measured at day 21. Root mean squared roughness (R_q) was also calculated using the WinROOF software. The number of pits per ROI was counted at day 21 and individual pit volumes (n=15 per material) were measured at day 21.

Statistics

Tests for equality of variance and normality were performed before using Analysis of variance (ANOVA) with Tukey's HSD post-hoc testing as necessary. Unless stated otherwise, ANOVA and Tukey's HSD post-hoc testing were used; otherwise a Kruskal-Wallis test was used with a

Wilcoxon-Mann-Whitney post-hoc test. Calculations were performed with JMP (SAS) software. Error bars in plots represent standard deviation except where indicated otherwise.

RESULTS

Materials characterisation

XRD traces revealed that HA, Si_{0.3}HA and Si_{0.5}HA samples were phase pure after heating to 1200 °C as shown in [Fig. 1]. The only phase present was ICDD No. 09-0432 for stoichiometric HA with a hexagonal crystal system. FTIR revealed major phosphate and hydroxyl peaks commonly reported for HA [Fig. 2].²⁵ Silicate peaks or shoulders were observed in SiHA [Fig. 2].^{26,27} No glassy silica Si-O-Si peaks were detected near 800 cm⁻¹, but orthosilicate peaks were observed suggesting that these groups were incorporated into the HA structure. XRF determined that the amount of silicon in Si_{0.3}HA and Si_{0.5}HA was 0.54 wt% and 1.17 wt% respectively [Table 1]. Measured Ca/P ratios were within ± 0.01 and Ca/P+Si ratios were within ± 0.02 of the calculated molar ratios [Table 1].

Soluble silicate and OC resorption of CaP coated discs

There was no significant effect of soluble silicate on cell viability as determined by the MTS assay [Fig. 3(A)] except at the highest concentration where 500 µm silicate showed a significantly lower absorbance than 0.05 µm silicate unlike the 500 mM NaOH control. Similarly there was no significant effect of silicate on osteoclast resorption of calcium phosphate when compared to the NaOH control with the exception of the highest concentration, 500 µm, where osteoclastic resorption was completely prevented [Fig. 3(B)].

OC formation on HA and SiHA

OC phenotypes were expressed on both HA and SiHA samples that were seeded with PBMCs and cultured for 14-21 days. CD14⁺ PBMCs seeded on permanox slides were TRAP positive [Fig. 4(A)] after 21 days, showing these cells were capable of displaying a marker frequently associated with OCs. Multinucleated cells with actin rings formed on all materials after 14 and 21 days [Fig. 4(B)]. OCs tended to form in plaques similarly observed by Spence et al. on HA and CHA discs *in vitro* compared to a more uniform distribution on dentine.¹² The presence of an actin ring and multiple nuclei is demonstrative of an OC phenotype,²⁸ so OC numbers were counted using this criteria. At day 14, HA and Si_{0.3}HA had significantly higher ($p < 0.01$ and $p < 0.05$ respectively) numbers of OCs compared to Si_{0.5}HA [Fig. 5(A)]. Day 21 values were significantly ($p < 0.05$) higher than day 14 values. Si_{0.5}HA OC numbers increased rapidly between days 14 and 21 to produce the largest mean value at day 21. However, there were no significant ($p < 0.05$) differences detected between OC numbers at day 21.

The morphology of the actin rings was different between HA and SiHA samples at day 21. SiHA discs favoured the formation of thicker and smaller OC sealing zones despite the similar OC numbers observed at day 21 shown in Fig. 5(A). HA had significantly larger ($p < 0.01$) diameter actin rings (130 μm vs. 60 μm) compared to Si_{0.3}HA and Si_{0.5}HA [Fig. 5(B)]. The mean actin ring thickness was larger (8 μm vs. 5 μm) on SiHA compared to HA discs [Fig. 5(C)].

***In vitro* OC resorption of HA and SiHA substrates**

Resorption area and volume measurements were performed on discs from two independent experiments. The resorption area was measured as a percentage of the total disc area from $n=4$ samples of each material. There were no significant ($p < 0.05$) differences between resorption area on HA, Si_{0.3}HA or Si_{0.5}HA at 11 or 21 days [Fig. 6]. The only significant ($p < 0.05$) difference in resorbed area was between Si_{0.5}HA at days 11 and 21. This finding corresponds to the lower

concentration of OCs observed on Si_{0.5}HA at 14 days as measured in a separate experiment [Fig.5(A)].

Volume measurements were made on n=5 samples with 3 ROIs (5 mm diameter) measured on each sample. The baseline means at day 0 for volume and R_q were similar and significantly lower (p<0.01) than the resorbed discs at day 21 as expected [Fig. 7(A-B)]. The mean volume of resorption at 21 days was slightly higher for Si_{0.5}HA compared to HA and Si_{0.3}HA, but there were no significant differences (p>0.05) between samples at day 21 [Fig. 7(A)]. R_q values also increased from day 0 to day 21 samples supporting the resorbed volume measurements [Fig. 7(B)]. The largest mean increase in volume between days 0 and 21 was Si_{0.5}HA with a change of 0.21 μm (volume.area⁻¹) compared to 0.16 μm and 0.15 μm for HA and Si_{0.3}HA respectively. The number of OC resorption pits on Si_{0.5}HA was lower (p<0.05) than on HA [Fig. 7(C)], but the mean individual pit volume was almost 4 fold higher on Si_{0.5}HA than on HA [Fig. 7(D)].

OC resorption areas corresponded to the plaque-like formation of OCs near the centre of the discs observed during fluorescence microscopy [Fig. 8(A)]. The resorption pits typically had a non-uniform depth [Fig. 8(B)], which necessitated the use of whole surface and individual pit volume measurements as opposed to simple measurement of pit depth. The pits highlighted in [Figs. 8(B-C) *Si_{0.3}HA, Si_{0.5}HA*] are likely the products of adjacent or migratory^{18,29} OCs that were shown to have ~60 μm sealing zones [Fig. 5(B)]. The resorption pit surfaces revealed an intergranular structure typical of synthetic CaPs that have been resorbed by OCs or subjected to local acidic attack [Fig. 8(C)].^{8,9}

DISCUSSION

The aim of this study was to determine whether silicate substitution in HA subsequently altered OC formation and resorption behaviour. Silicon substitution induces chemical and structural changes in HA that lead to changes in the *in vitro* OC response as previously suggested in studies by Botelho et al. and Lehmann et al.^{11,16} OC numbers, actin ring morphology and OC resorption pits are important measures of OC development and activity that have not yet been investigated on phase pure SiHA. Phase purity was important for this experiment because secondary phases could alter the silicate and calcium solubility. It then becomes difficult to draw conclusions about whether an OC response was due to SiHA or a secondary phase, such as CaO or TCP.

SiHA was characterised in this study to confirm phase purity, stoichiometry and the presence of silicate ions in HA. The adjusted Ca/P ratio mentioned in the ‘Materials production’ section was necessary to obtain phase pure SiHA samples at 1200 °C [Fig. 1]. This was due to slightly lower Si amounts [Table 1] in SiHA as measured with XRF compared to the expected stoichiometric Ca/P+Si ratios. The decreased Si amounts here are likely the result of incomplete hydrolysis of TEOS and inadvertent atmospheric carbonate substitution at room temperature.³⁰ Glassy silica (Si-O-Si), undetectable in XRD at low levels, can form in SiHA with larger Si amounts ($x=0.75$ or more) or when using non-aqueous methods of synthesis.²⁶ Such entities could unknowingly impact the outcome of biological studies but were not observed here [Fig. 2].

OC formation on synthetic HA and SiHA

The chemistry (including substituting ions such as Zn),³¹ surface energy,³² solubility⁸ and topography³³ of materials are all known to impact OC formation and adhesion, which can regulate sealing zone architecture and dynamics.³⁴ All disc surfaces were polished and grain size differences were not of a magnitude known to alter OC behaviour so topography was controlled

for.³⁵ Our findings regarding OC formation on SiHA [Fig. 4] agree with Botelho et al. who showed that OCs can form on synthetic Si_{0.3}HA, Si_{0.5}HA and HA substrates from CD14+ PBMCs with co-localisation of vinculin and actin, indicative of sealing zone formation.¹¹

The delayed formation of OCs from PBMCs on Si_{0.5}HA at day 14 [Fig.5 (A)] was probably due to differences in surface charge³² and / or solubility.³⁶ Matesanz et al. also reported inhibited OC formation after 21 days on nSiHA (0.8 wt%) compared to nHA.¹⁷ However, they also reported that the viability of RAW 264.7 murine macrophages was not reduced in SiHA compared to HA. The use of murine macrophages, lower concentrations of RANKL and a more soluble nano grained nSiHA, could explain the temporal differences between their study and this one (reduced OC formation on Si_{0.5}HA at 14 days instead of 21 days) [Fig.5 (A)].

Soluble Si did not show any adverse metabolic effects under 500 µM Si on PBMCs at 3 days on osteologic CaP substrates [Fig. 3(A)] or on [3-100 µM] RAW 254.7 OCs on tissue culture plastic at 3 days.¹⁴ However, at 500 µM Si OC metabolic activity and resorption activity on CaP substrates declined [Fig.3]. Similar concentrations of soluble Si (from dissolved bioglass 45S5 particles) of ~690 µM inhibited OC formation (RAW254.7) and resorption of murine calvarial bone *in vitro*.¹⁵ Ca was likely the dominant factor in any solubility-mediated influence Si_{0.3}HA and particularly Si_{0.5}HA had at later time points (day 21) in this study.³⁷ Hayakawa et al. found a non-linear increase in Ca release from SiHA with increasing Si amounts under acidic conditions (pH 4.0).³⁸ Early burst style release of higher Si amounts from Si_{0.5}HA, a passive effect (altered surface charge due Si substitution) higher amounts of extracellular Ca or a slightly higher pH (above 7.30 pH) could explain the reduced OC numbers and resorption activity at day 14 for Si_{0.5}HA, and medium changes coupled with decreasing non-steady state Si release might

have reduced the effects of Si at day 21 [Figs. 5(A) and 6].^{37,39,40} However, Ca and Si release from SiHA was not quantified in this study because this would not account for re-precipitation of soluble Ca, P and or Si on the disc surface.

Apatitic matrix can promote sealing zone formation via cellular signalling,⁴¹ but the actin ring morphology can vary with subtle changes to stoichiometry or substituting ions. OCs tend to form smaller diameter, thicker and more stable actin rings on bone slices and CHA *in vitro* compared to other substrates such as stoichiometric HA, calcite and tissue culture plastic.^{9,18} The actin ring thicknesses and diameters on SiHA and HA [Fig. 5(B-C)] was comparable to those observed on crystalline CHA (8.9 wt% CO₃) and HA respectively seen in a separate study.⁹ The smaller and thicker actin rings on Si_{0.3}HA and Si_{0.5}HA compared to HA [Figs. 5(B-C)] denote actin morphology indicative of increased sealing zone integrity that could encourage OC resorption. Changes to extracellular ligands that affect actin ring structure could be due to both material solubility and material surface chemistry. SiHA is known to have a higher binding affinity for collagen,⁴² and a collagenous matrix is important for OC actin ring formation.⁴³ Botelho et al. theorized that this phenomenon could lead to enhanced OC resorption activity.¹¹

OC resorption activity on HA and SiHA

While smaller and more stable sealing zone morphologies can promote resorption, the rate and morphology of OC resorption also depends on material properties such as chemistry, solubility and surface area in addition to extracellular pH.^{18,39,40} Dense crystalline discs were used in this study in an attempt to 1) reduce the effects of surface area and 2) allow for consistent confocal pit measurement. Yamada et al. highlighted the importance of volume measurements of OC pits in their study that showed significant differences in pit depth and pit volume between TCP and

ZnTCP, but no difference in the pit area.¹⁰ New confocal imaging techniques have enabled the measurement of pit depth, which is frequently non-uniform [Fig. 7(B)], and resorption volume. Our findings support a mechanism where Si_{0.5}HA was more susceptible to dissolution in a localized low pH (3-4) environment due to increased triple point junctions³⁶ as opposed to earlier OC differentiation from CD14+ PBMCs as observed by Nakamura et al. (15-18 days).⁹ Small changes in extracellular pH (as low as 0.10 units between 7.15 and 7.25 pH) can promote or inhibit OC resorption.^{39,40} The local environment around OCs on SiHA is complex due to possible modulation of extracellular pH resulting from the basic dissolution products of SiHA. Extracellular pH cannot be excluded as a possible mechanism of enhanced OC resorption here.

Once OCs developed on Si_{0.5}HA, there were fewer pits on its surface with larger individual pit volumes than on HA [Fig. 7(C,D)], but whole disc area and ROI (20 mm²) volume measurements didn't show any significant differences despite slightly elevated means for Si_{0.5}HA at 21 days [Figs. 6 & 7(A)]. The reduced pit numbers with larger pit volumes seen with Si_{0.5}HA was not due to shallower pits with a larger surface area as both Si_{0.3}HA and Si_{0.5}HA showed smaller, well defined pit borders [Fig. 8 (A)] that support the smaller actin ring diameters discussed earlier [Fig. 6 (B)]. Therefore the reduced pit numbers per area on Si_{0.5}HA, despite larger individual pit volume, likely contributed to a false negative error in ROI volume at 21 days [Fig. 7(A, C)]. The larger volume pits with fewer pit numbers on Si_{0.5}HA might indicate a preferred *in vitro* OC resorption mechanism (i.e., tunnelling vs. trough (migratory) resorption). Resting or migrating OCs can be inhibited with increased extracellular Ca concentrations,³⁷ so the deeper individual pit volumes on Si_{0.5}HA [Fig. 7(D)] indicate a preference for active resorption as opposed to migration.⁴¹ The SiHA resorption surfaces also exhibited a more

‘etched’ surface clearly exposing grains compared to a HA where grains were not exposed as clearly [Fig. 8]. This further supports a solubility mediated OC resorption on SiHA.

Complementary reports of OC resorption of SiHA support our findings. The increased Ca and P release from Si_{0.5}HA cultured with OCs *in vitro* for 21 days shown by Botelho et al. also suggests an increased susceptibility of Si_{0.5}HA to acidic OC attack.¹¹ However, Si release was not measured here and the possibility of CaP re-precipitation at the HA or SiHA interface was not considered. Re-precipitation in Botelho’s study would have only decreased soluble Ca and P differences between SiHA with OCs and the control (SiHA only). Lehmann et al. observed increased numbers of resorption lacunae on Si_{0.5}HA compared to HA, but their SiHA also contained the more soluble α -TCP phase.¹⁶ Matesanz et al. observed smaller diameter lacunae on nSi_{0.3}HA compared to nHA suggesting a possible reduction in OC activity, but they did not report pit numbers or depth information.¹⁷

Although minor increases in CaP lattice solubility may encourage more aggressive OC resorption, high amounts of dissolution can have an inverse effect. The work of Detsch et al. found that HA was more aggressively resorbed by OCs compared to a more soluble β -TCP.⁸ Studies investigating OB-OC cross talk could reveal whether signalling and/or OC resorption is altered in the presence of SiHA. However, one suspected mechanism of enhanced bone formation in porous SiHA *in vivo* was increased remodelling at the tissue/implant surface compared to HA⁷ requiring a positive effect of SiHA on osteoclast resorption and osteoblast activity.

CONCLUSIONS

New *in vitro* osteoclastogenesis and resorption metrics were used to study the effects of soluble Si and SiHA on OCs. Soluble Si under 500 μM did not alter OC metabolic activity or resorption on CaP coated discs. Higher initial Si release rates might explain early OC inhibition on $\text{Si}_{0.5}\text{HA}$, but structurally induced changes in HA due to Si substitution could explain late resorption activity on $\text{Si}_{0.3}\text{HA}$ and $\text{Si}_{0.5}\text{HA}$. The smaller and thicker actin ring morphologies on SiHA were likely due to both surface energy and solubility differences compared to HA. The larger individual pit volumes and delayed OC formation on $\text{Si}_{0.5}\text{HA}$ suggested increased lattice solubility as opposed to earlier OC differentiation as a mechanism for enhanced OC resorption. Although recent studies have suggested reduced OC activity as a result of Si, the form (soluble monomer, amorphous silica or lattice bound) and amount must be carefully evaluated, as these trends were not observed in this study for $\text{Si}_{0.3}\text{HA}$ or $\text{Si}_{0.5}\text{HA}$.^{15,17}

ACKNOWLEDGEMENTS

This work was supported by a National Science Foundation Graduate Research Fellowship (RJF) (DGE-1042796) and a Cambridge International Scholarship from the Cambridge Overseas Trusts (RJF). RAB acknowledges funding support from the National Institute for Health Research.

REFERENCES

1. Boyan BD, Schwartz Z, Lohmann CH, Sylvia VL, Cochran DL, Dean DD, et al. Pretreatment of bone with osteoclasts affects phenotypic expression of osteoblast-like cells. *J Orthop Res.* 2003;21(4):638–47.
2. Spence G, Patel N, Brooks R, Rushton N. Carbonate substituted hydroxyapatite: Resorption by osteoclasts modifies the osteoblastic response. *J Biomed Mater Res Part A.* 2009;90A(1):217–24.
3. Spence G, Phillips S, Champion C, Brooks R, Rushton N. Bone formation in a carbonate-substituted hydroxyapatite implant is inhibited by zoledronate The importance of bioresorption to osteoconduction. *J Bone Jt Surgery-British Vol.* 2008;90B(12):1635–40.

4. Tonino AJ, Thèrin M, Doyle C. Hydroxyapatite-coated femoral stems: Histology and histomorphometry around five components retrieved at post mortem. *J Bone Jt Surgery, Br Vol.* 1999 Jan 1;81-B(1):148–54.
5. Brooks RA, Field RE, Jones E, Sood A, Rushton N. A histological study of retrieved Cambridge acetabular components. *Hip Int.* 72/74 Via Fruili, 20135 Milan, Italy: Wichtig Editore; 2010;20(1):56–63.
6. Patel N, Brooks RA, Clarke MT, Lee PMT, Rushton N, Gibson IR, et al. In vivo assessment of hydroxyapatite and silicate-substituted hydroxyapatite granules using an ovine defect model. *J Mater Sci Med.* 2005;16(5):429–40.
7. Hing KA, Revell PA, Smith N, Buckland T. Effect of silicon level on rate, quality and progression of bone healing within silicate-substituted porous hydroxyapatite scaffolds. *Biomaterials.* 2006 Oct;27(29):5014–26.
8. Detsch R, Mayr H, Ziegler G. Formation of osteoclast-like cells on HA and TCP ceramics. *Acta Biomater.* 2008 Jan;4(1):139–48.
9. Nakamura M, Hentunen T, Salonen J, Nagai A, Yamashita K. Characterization of bone mineral-resembling biomaterials for optimizing human osteoclast differentiation and resorption. *J Biomed Mater Res A.* 2013 Nov;101(11):3141–51.
10. Yamada Y, Ito A, Kojima H, Sakane M, Miyakawa S, Uemura T, et al. Inhibitory effect of Zn²⁺ in zinc-containing beta-tricalcium phosphate on resorbing activity of mature osteoclasts. *J Biomed Mater Res A.* 2008 Feb;84(2):344–52.
11. Botelho CM, Brooks RA, Spence G, McFarlane I, Lopes MA, Best SM, et al. Differentiation of mononuclear precursors into osteoclasts on the surface of Si-substituted hydroxyapatite. *J Biomed Mater Res Part A.* 2006;78A(4):709–20.
12. Spence G, Patel N, Brooks R, Bonfield W, Rushton N. Osteoclastogenesis on hydroxyapatite ceramics: The effect of carbonate substitution. *J Biomed Mater Res Part A.* 2008;92A(4):1292–300.
13. Porter AE, Patel N, Skepper JN, Best SM, Bonfield W. Effect of sintered silicate-substituted hydroxyapatite on remodelling processes at the bone-implant interface. *Biomaterials.* 2004 Jul;25(16):3303–14.
14. Schroder HC, Wang XH, Wiens M, Diehl-Seifert B, Kropf K, Schlossmacher U, et al. Silicate Modulates the Cross-Talk Between Osteoblasts (SaOS-2) and Osteoclasts (RAW 264.7 Cells): Inhibition of Osteoclast Growth and Differentiation. *J Cell Biochem.* 2012;113(10):3197–206.

15. Mladenović Ž, Johansson A, Willman B, Shahabi K, Björn E, Ransjö M. Soluble silica inhibits osteoclast formation and bone resorption in vitro. *Acta Biomater.* 2014 Jan;10(1):406–18.
16. Lehmann G, Cacciotti I, Palmero P, Montanaro L, Bianco A, Campagnolo L, et al. Differentiation of osteoblast and osteoclast precursors on pure and silicon-substituted synthesized hydroxyapatites. *Biomed Mater.* 2012 Oct;7(5):055001.
17. Matesanz MC, Linares J, Lilue I, Sánchez-Salcedo S, Feito MJ, Arcos D, et al. Nanocrystalline silicon substituted hydroxyapatite effects on osteoclast differentiation and resorptive activity. *J Mater Chem B.* 2014;2(19):2910.
18. Geblinger D, Geiger B, Addadi L. Surface-induced regulation of podosome organization and dynamics in cultured osteoclasts. *Chembiochem.* 2009 Jan 5;10(1):158–65.
19. Jarcho M, Bolen CH, Thomas MB, Bobick J, Kay JF, Doremus RH. Hydroxylapatite synthesis and Characterization in dense polycrystalline form. *J Mater Sci.* 1976;11(11):2027–35.
20. Kim SR, Lee JH, Kim YT, Riu DH, Jung SJ, Lee YJ, et al. Synthesis of Si, Mg substituted hydroxyapatites and their sintering behaviors. *Biomaterials.* 2003;24(8):1389–98.
21. Gibson IR, Best SM, Bonfield W. Chemical characterization of silicon-substituted hydroxyapatite. *J Biomed Mater Res.* 1999;44(4):422–8.
22. Schilling AF, Linhart W, Filke S, Gebauer M, Schinke T, Rueger JM, et al. Resorbability of bone substitute biomaterials by human osteoclasts. *Biomaterials.* 2004;25(18):3963–72.
23. Susi F, Goldhabe P, Jennings J. Histochemical and biochemical study of acid phosphatase in resorbing bone in culture. *Am J Physiol. American Physiological Society;* 1966 Oct;211(4):959–62.
24. Farquharson C, Whitehead C, Rennie S, Thorp B, Loveridge N. Cell proliferation and enzyme activities associated with the development of avian tibial dyschondroplasia: An in situ biochemical study. *Bone.* 1992;13(1):59–67.
25. Koutsopoulos S. Synthesis and characterization of hydroxyapatite crystals: A review study on the analytical methods. *J Biomed Mater Res.* 2002;62(4):600–12.
26. Marchat D, Zymelka M, Coelho C, Gremillard L, Joly-Pottuz L, Babonneau F, et al. Accurate characterization of pure silicon-substituted hydroxyapatite powders synthesized by a new precipitation route. *Acta Biomater.* 2013 Jun;9(6):6992–7004.
27. Hayakawa S, Hench LL. AM1 study on infra-red spectra of silica clusters modified by fluorine. *J Non Cryst Solids.* 2000;262(1):264–70.

28. Monchau F, Lefèvre A, Descamps M, Belquin-myrdycz A, Laffargue P, Hildebrand H. In vitro studies of human and rat osteoclast activity on hydroxyapatite, β -tricalcium phosphate, calcium carbonate. *Biomol Eng.* 2002 Aug;19(2-6):143–52.
29. Vaananen H, Zhao H, Mulari M, Halleen J. The cell biology of osteoclast function. *J Cell Sci.* 2000 Feb 1;113(3):377–81.
30. Palard M, Champion E, Foucaud S. Synthesis of silicated hydroxyapatite $\text{Ca}_{10}(\text{PO}_4)_6-x(\text{SiO}_4)_x(\text{OH})_{2-x}$. *J Solid State Chem.* 2008 Aug;181(8):1950–60.
31. Kishi S, Yamaguchi M. Inhibitory effect of zinc compounds on osteoclast-like cell formation in mouse marrow cultures. *Biochem Pharmacol.* 1994 Sep;48(6):1225–30.
32. Vandiver J, Dean D, Patel N, Botelho C, Best S, Santos JD, et al. Silicon addition to hydroxyapatite increases nanoscale electrostatic, van der Waals, and adhesive interactions. *J Biomed Mater Res Part A.* 2006;78A(2):352–63.
33. Brinkmann J, Hefti T, Schlottig F, Spencer ND, Hall H. Response of osteoclasts to titanium surfaces with increasing surface roughness: an in vitro study. *Biointerphases.* 2012 Dec;7(1-4):34.
34. Anderegg F, Geblinger D, Horvath P, Charnley M, Textor M, Addadi L, et al. Substrate Adhesion Regulates Sealing Zone Architecture and Dynamics in Cultured Osteoclasts. *PLoS One.* 2011;6(12).
35. Webster TJ, Ergun C, Doremus RH, Siegel RW, Bizios R. Enhanced osteoclast-like cell functions on nanophase ceramics. *Biomaterials.* 2001;22(11):1327–33.
36. Porter AE, Patel N, Skepper JN, Best SM, Bonfield W. Comparison of in vivo dissolution processes in hydroxyapatite and silicon-substituted hydroxyapatite bioceramics. *Biomaterials.* 2003 Nov;24(25):4609–20.
37. Lakkakorpi PT, Lehenkari PP, Rautiala TJ, Väänänen HK. Different calcium sensitivity in osteoclasts on glass and on bone and maintenance of cytoskeletal structures on bone in the presence of high extracellular calcium. *J Cell Physiol.* 1996 Sep;168(3):668–77.
38. Hayakawa S, Kanaya T, Tsuru K, Shirotsaki Y, Osaka A, Fujii E, et al. Heterogeneous structure and in vitro degradation behavior of wet-chemically derived nanocrystalline silicon-containing hydroxyapatite particles. *Acta Biomater.* 2012/08/28 ed. 2013 Jan;9(1):4856–67.
39. Arnett TR, Spowage M. Modulation of the resorptive activity of rat osteoclasts by small changes in extracellular pH near the physiological range. *Bone.* 1996;18(3):277–9.
40. Arnett TR. Extracellular pH regulates bone cell function. *J Nutr.* 2008;138(2):415S – 418S.

41. Saltel F, Destaing O, Bard F, Eichert D, Jurdic P. Apatite-mediated actin dynamics in resorbing osteoclasts. *Mol Biol Cell. Amer Soc Cell Biology*; 2004 Dec;15(12):5231–41.
42. Botelho CM, Brooks RA, Kawai T, Ogata S, Ohtsuki C, Best SM, et al. In vitro analysis of protein adhesion to phase pure hydroxyapatite and silicon substituted hydroxyapatite. In: Li P, Zhang K, Colwell CW, editors. *Bioceramics 17*. Zurich-Uetikon: Trans Tech Publications Ltd; 2005. p. 461–4.
43. Teitelbaum SL. Bone Resorption by Osteoclasts. *Science (80-)*. 2000 Sep 1;289(5484):1504–8.

TABLE 1. Calculated and XRF measured Ca/P, Ca/P+Si ratios and Si amounts.

Sample	Ca/P		Ca/P+Si		wt% Si	
	<i>expected</i>	<i>measured</i>	<i>expected</i>	<i>measured</i>	<i>expected</i>	<i>measured</i>
HA	1.67	1.66				
Si _{0.3} HA	1.75	1.75	1.67	1.69	0.85	0.54
Si _{0.5} HA	1.81	1.82	1.67	1.68	1.50	1.17

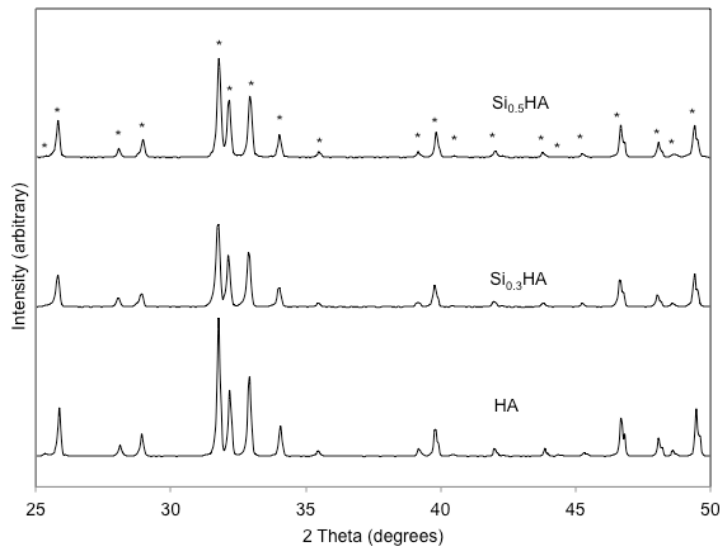


FIGURE 1. XRD reflections of HA, Si_{0.3}HA and Si_{0.5}HA heated to 1200 °C. * Indicates ICDD # 09-0432 peaks. Major impurity peaks occur over the 25-50° 2θ.

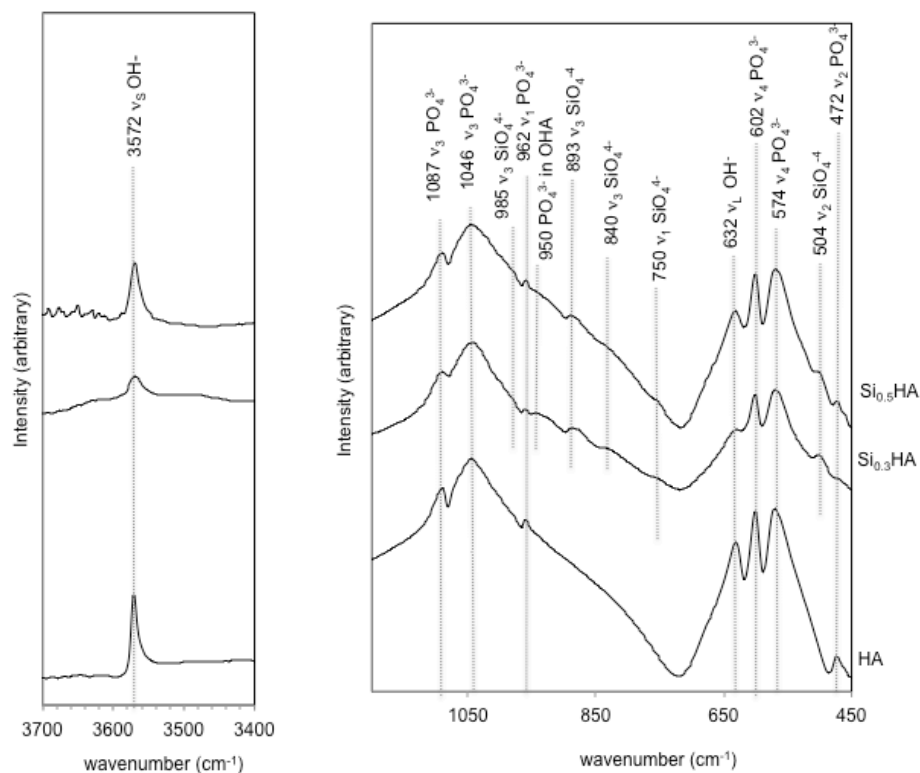


FIGURE 2. FTIR scans of heat treated HA and SiHA (1200 °C). The region from 1200-450 cm^{-1} was enhanced to highlight major phosphate, hydroxyl and silicate peaks typical for HA and SiHA. SiHA had an oxyhydroxyapatite peak near 950 cm^{-1} . The enhanced region from 3700-3400 cm^{-1} highlights the characteristic hydroxyl-stretching peak.

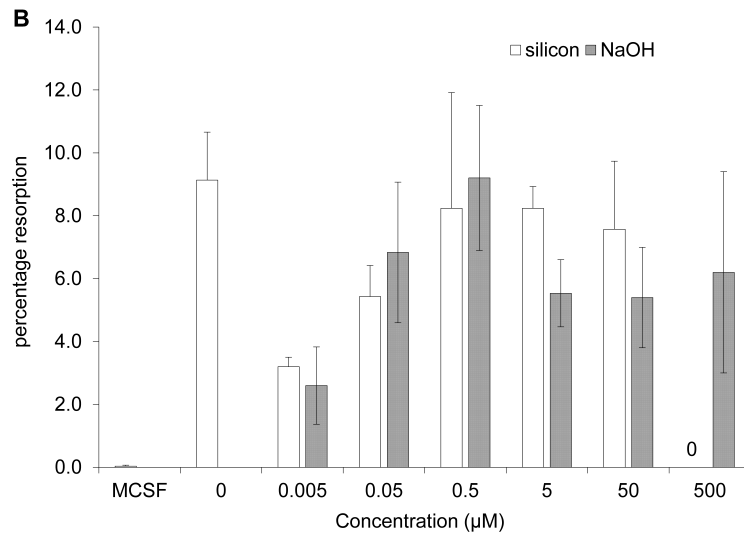
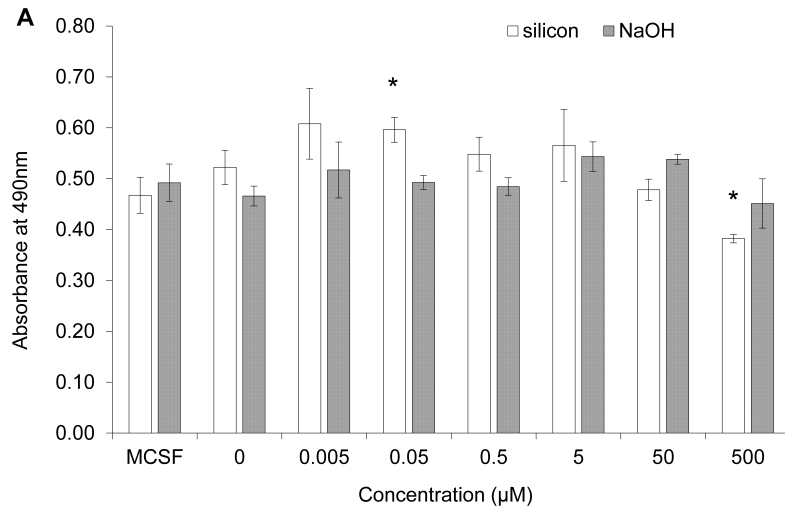


FIGURE 3. (A) Cellular metabolism as represented by reduction of MTS dye after 4 days in the presence of silicate or NaOH (control) and (B) area resorption as a result of 0.005-500 µM silicon in the culture medium after 7 days. Values are mean ± s.d.; n=3 for A and mean ± S.E.M.; n=3 for B.

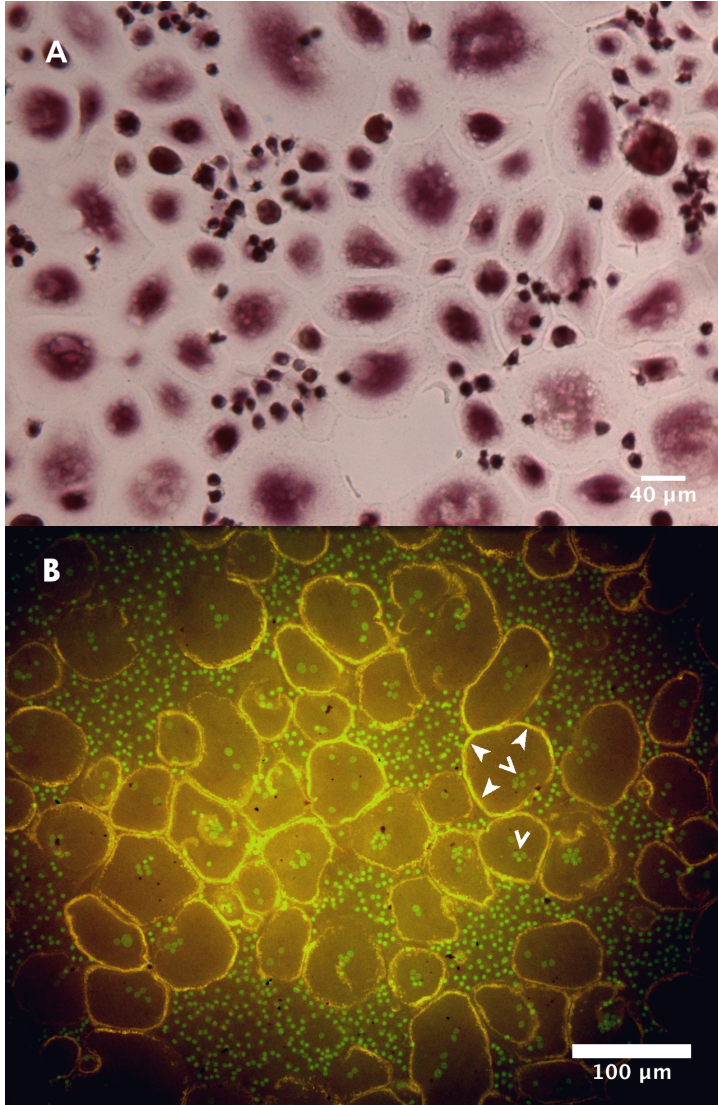


FIGURE 4. TRAP positive multinucleated cells generated from CD14+ PBMCs after 21 days (A). Fluorescence image of nuclei (blue/green) and actin rings (red/yellow) typical of an OC after 21 days *in vitro* on SiHA0.5 (B). The closed arrowheads point towards an actin ring and the open headed arrowheads point towards cell nuclei.

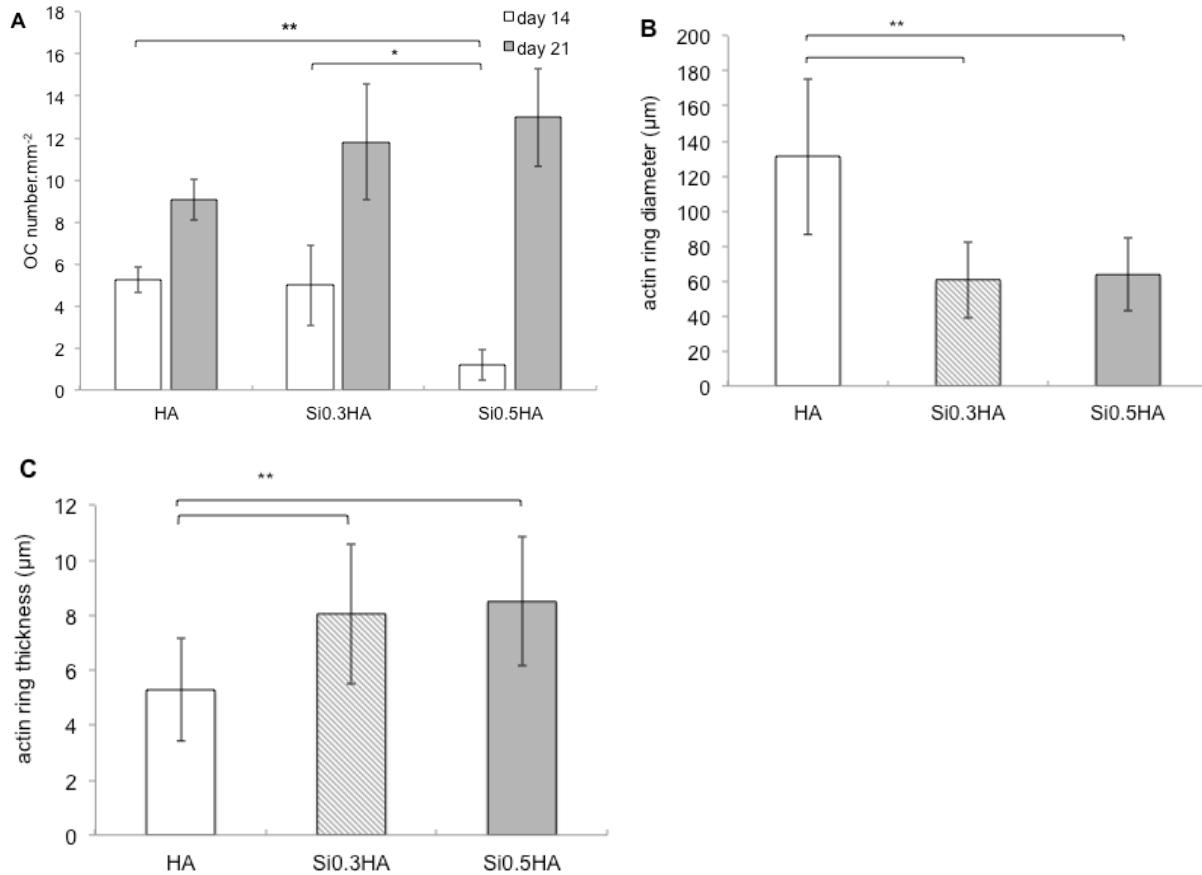


FIGURE 5. (A) OC numbers counted from fluorescence mosaic images (n=6 samples per condition) after 14 and 21 days on HA, Si_{0.3}HA and Si_{0.5}HA. An OC was considered to have at least 3 nuclei and an actin ring. (B) Actin ring diameters were measured at day 21 from n=6 samples per condition (50 ring diameters per sample). (C) Actin ring thicknesses were measured at day 21 from n=6 samples per condition (50 thicknesses per sample). Error bars for all plots represent s.d. * denotes p<0.05 and ** p<0.01.

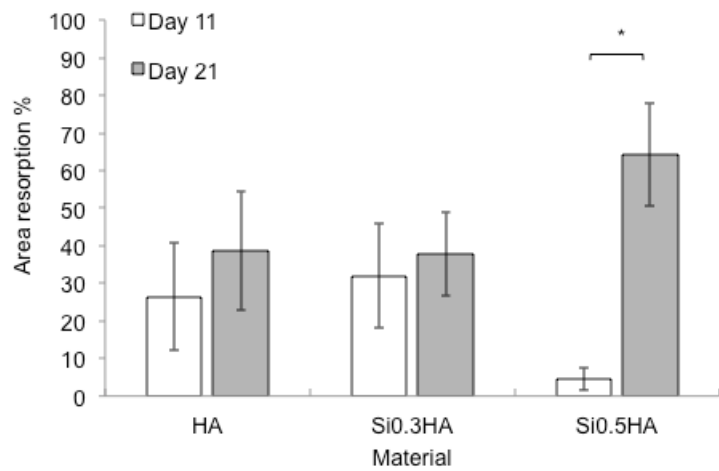


FIGURE 6. Area resorption as measured by thresholding in Image J (n=4). The only significant difference found (* p<0.05) was between areas measured at days 11 and 21 for Si_{0.5}HA. These measurements were obtained from an independent experiment from those obtained in Figures 5 and 7.

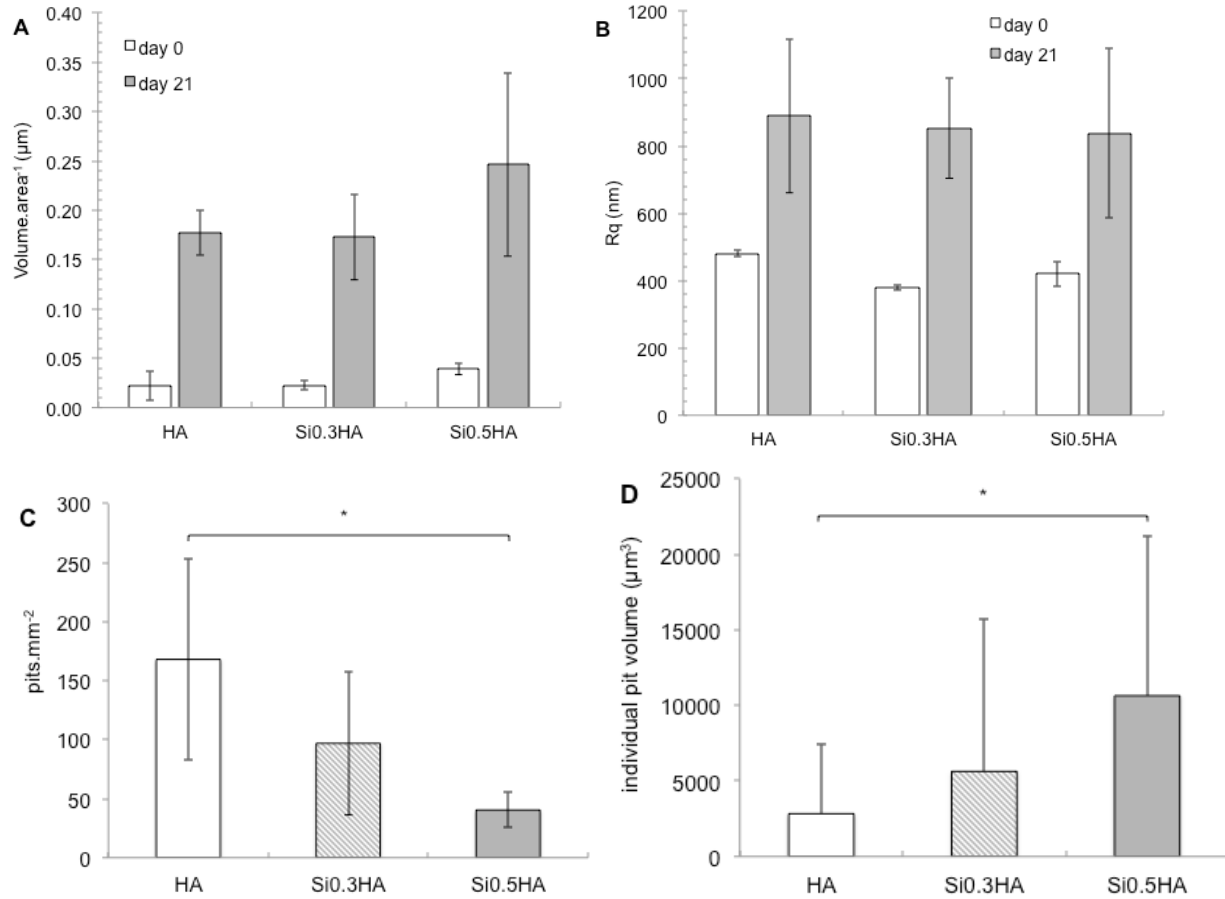
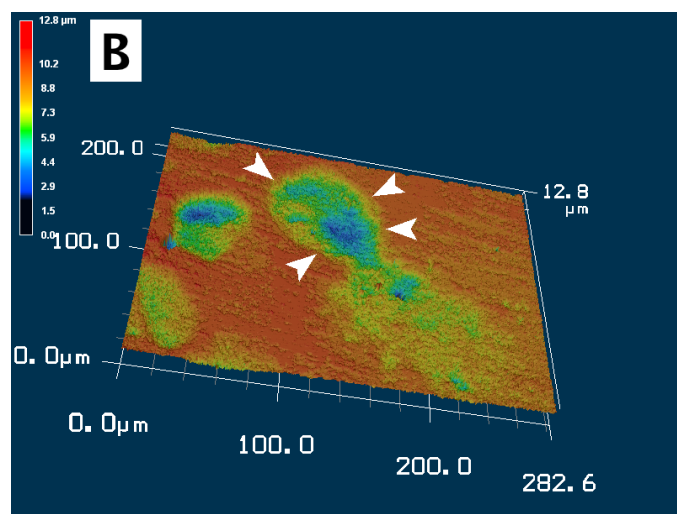
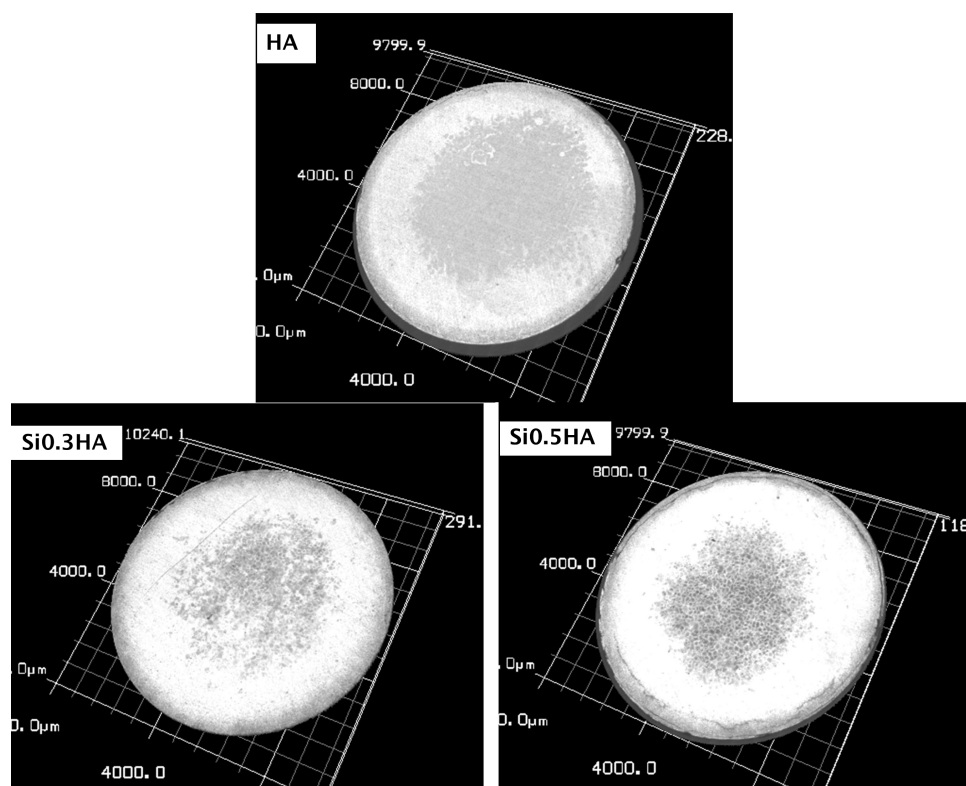


FIGURE 7. (A) Mean volume resorption per ROI (20 mm²) from n=5 samples per condition (3 ROIs per disc) before and after *in vitro* OC culture for 21 days. No differences were detected between materials, but differences between measurements at day 0 and 21 were significant (p<0.01). (B) Roughness values R_q obtained from traces along the ROIs measured in 3D laser microscopy and calculated using the WinROOF software. Again no differences between materials were observed, but R_q significantly (p<0.01) increased between day 0 and day 21. (C) Number of resorption pits per ROI from n=5 samples per condition (3 ROIs per disc) at 21 days. (D) Individual OC pit volumes (n=15 per material) after 21 days. A Kruskal-Wallis and a Mann-Whitney U post-hoc test were used.

[A]



[C]

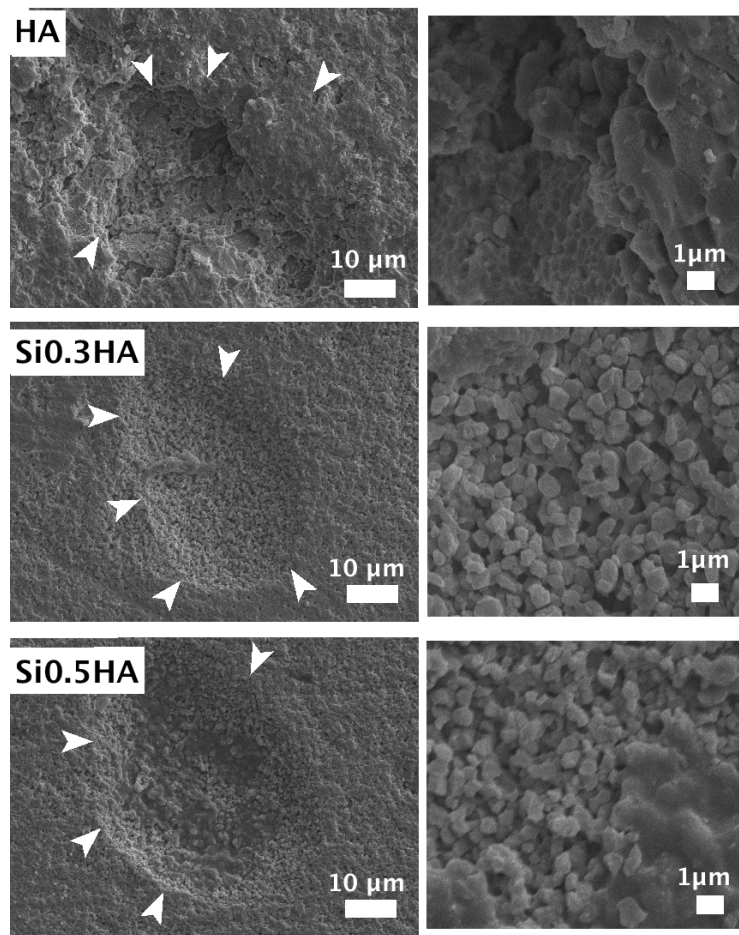


FIGURE 8. (A) Macroscale images of OC resorption on the sample surfaces after 21 days. (B) Laser image of a resorption pit on Si_{0.5}HA after 21 days. This confocal image shows the non-uniform morphology typical of OC pits. (C) SEM images of HA, Si_{0.3}HA and Si_{0.5}HA surfaces after 21 days with arrowheads indicating an OC resorption pit.